

A Test of the Copernican Principle

R. R. Caldwell¹ and A. Stebbins²

¹*Department of Physics & Astronomy, 6127 Wilder Lab, Dartmouth College, Hanover, NH 03755*

²*Theoretical Astrophysics Group, Fermi National Accelerator Laboratory, P.O. Box 500, Batavia, IL 60510*

(Dated: October 22, 2018)

The blackbody nature of the cosmic microwave background (CMB) radiation spectrum is used in a modern test of the Copernican Principle. The reionized universe serves as a mirror to reflect CMB photons, thereby permitting a view of ourselves and the local gravitational potential. By comparing with measurements of the CMB spectrum, a limit is placed on the possibility that we occupy a privileged location, residing at the center of a large void. The Hubble diagram inferred from lines-of-sight originating at the center of the void may be misinterpreted to indicate cosmic acceleration. Current limits on spectral distortions are shown to exclude the largest voids which mimic cosmic acceleration. More sensitive measurements of the CMB spectrum could prove the existence of such a void or confirm the validity of the Copernican Principle.

Introduction: The observed accelerating expansion of the universe [1, 2] poses deep questions for cosmology. Is the universe filled by some new, exotic dark energy, or is one of the basic tenets of the standard model of cosmology invalid? One such tenet is the Cosmological Principle, the assumption of approximate homogeneity and isotropy of matter and radiation throughout the universe. The Cosmological Principle is known to be partly satisfied. The universe is observed to be very nearly isotropic on our celestial sphere, on the basis of the near-isotropy of the CMB temperature pattern [3]. The universe is observed to be approximately homogeneous across the distances probed by large-scale structures [4]. Yet, radial homogeneity on cosmic scales $\gtrsim 1$ Gpc remains to be proven. If the assumption of radial homogeneity is relaxed, and if we observe from a preferred vantage point, then it may be possible to explain the apparent cosmic acceleration in terms of a peculiar distribution of matter centered upon our location [5]. In fact, models of the universe consisting of a spherically-symmetric distribution of matter, mathematically described by a Lemaitre-Tolman-Bondi spacetime [6], have been shown to produce a Hubble diagram which is consistent with observations. These models require no cosmological constant or other form of dark energy, and locally resemble a matter-dominated low-density universe or void. The observed near-isotropy constrains us to occupy a very special location, at or near the center of the void, in violation of the Copernican Principle. Although the Copernican Principle may be widely accepted by *fiat*, it is imperative that such a foundational principle be proven.

We propose a test of the Copernican Principle, to verify radial homogeneity and thereby constrain non-accelerating void cosmological models. The test relies on a previously under-appreciated effect: the mixture of anisotropic CMB radiation through scattering leads to distortions of the blackbody spectrum [7]. The CMB is initially thermal (blackbody), but small inhomogeneities cause variations in the temperature at different locations and along different lines-of-sight that preserve the black-

body spectrum. However, scattering of this anisotropic radiation into our line-of-sight by ionized gas produces observable spectral distortions. This allows us to indirectly detect large anisotropies in other parts of the universe.

Here we are interested in anisotropies caused by a large, local void. Such a structure causes ionized gas to move outward, in motion relative to the CMB frame which leads to a Doppler anisotropy in the gas frame. The gravitational potential of such a structure also leads to a Sachs-Wolfe (SW) effect for photons which originate inside of the void and scatter back toward us. The geometry of these effects is illustrated in fig. 1. A large void, or any other non-Copernican structure, will lead to large anisotropies in other places which will be reflected back at us in the form of spectral distortions. Hence, deviations from a blackbody spectrum can indicate a violation of the Copernican Principle. In essence, we use the reionized universe as a mirror to look at ourselves in CMB light. If we see ourselves in the the mirror it is because ours is a privileged location. If we see nothing in the mirror, then the Copernican Principle is upheld.

Spectral Distortions: The distortion of the CMB blackbody spectrum due to scattering by anisotropic CMB radiation is [7] $u[\hat{\mathbf{n}}] = \frac{3}{16\pi} \int_0^\infty dz \frac{d\tau}{dz} \int d^2\hat{\mathbf{n}}' (1 + (\hat{\mathbf{n}} \cdot \hat{\mathbf{n}}')^2) \times \left(\frac{\Delta T}{T}[\hat{\mathbf{n}}, \hat{\mathbf{n}}, z] - \frac{\Delta T}{T}[\hat{\mathbf{n}}', \hat{\mathbf{n}}, z] \right)^2$, where $\Delta T/T[\hat{\mathbf{n}}', \hat{\mathbf{n}}, z]$ is the CMB temperature anisotropy in the direction $\hat{\mathbf{n}}'$, as observed at redshift z in the direction $\hat{\mathbf{n}}$ from the central observer, and τ is the optical depth. For cosmic voids extending out to redshifts $z \lesssim 1$, reflections back at us may occur up to $z \lesssim 3$ (see fig. 1). The optical depth to Thomson scattering is small, so that it is appropriate to consider single scattering. Since the mean CMB temperature is not known *a priori*, but rather is fit to the observations, u is observationally degenerate with the Compton y -distortion parameter according to the relation $u = 2y$. (Compare Refs. [7, 8] for details.) Thus observational constraints on $2y$ can be treated as constraints on u .

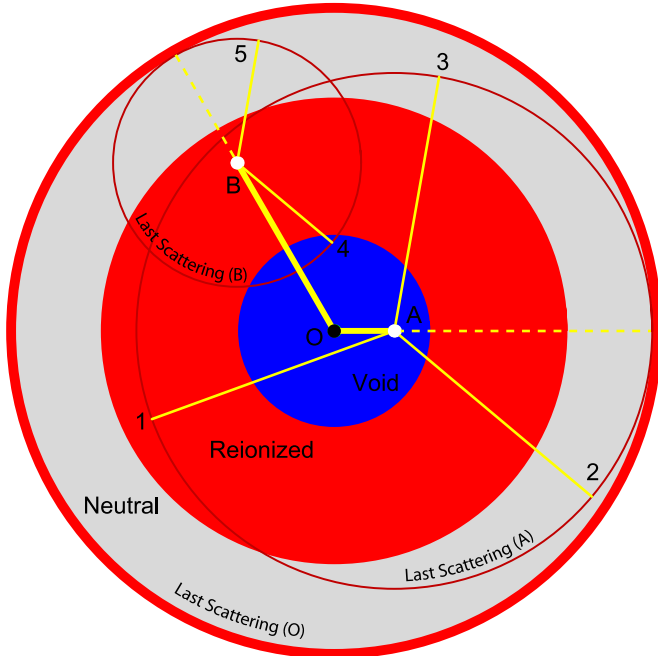


FIG. 1: Illustrated is a cross-section through a model universe with the observer (O) at the center of a void, in violation of the Copernican Principle. CMB photons traveling in any direction may Thomson scatter off reionized gas toward the observer. The final spectrum of the observed light will be a mixture of blackbody spectra with different (anisotropic) temperatures, producing a distorted blackbody. The yellow lines represent: incoming beams of unscattered, primary CMB photons (dashed); incoming beams of scattered photons (thin), and the observed beams (thick) for representative scattering centers with last scattering surfaces represented by the dark circles. A is in the *Doppler zone*: Beams 1-3 experience the same SW temperature shift, introducing no anisotropy. However, gradients in the void gravitational potential cause the gas to move with respect to the CMB frame, so A sees a differential Doppler anisotropy, resulting in spectral distortions. B is in the *reflection zone*: B is at rest with respect to the CMB frame and sees no Doppler anisotropy. However, some of the incoming photons, *e.g.* beam 4, originate inside the void so there will be an anisotropic SW temperature shift, leading to spectral distortions.

We consider a low-amplitude void embedded in a flat, Einstein-deSitter (EdS or $\Omega = 1$) matter-dominated universe. The gravitational potential due to the void, $\Phi[\mathbf{x}]$, is a function of comoving position, \mathbf{x} , with Earth near $\mathbf{x} = 0$. The temperature anisotropy can be divided into a Sachs-Wolfe and Doppler term $\frac{\Delta T}{T}[\hat{\mathbf{n}}', \hat{\mathbf{n}}, z] = \frac{\Delta T}{T}|_{\text{SW}} + \frac{\Delta T}{T}|_{\text{Doppler}}$ where $\frac{\Delta T}{T}|_{\text{SW}} = \frac{1}{3c^2}(\Phi[\mathbf{x}_{\text{rec}}] - \Phi[\mathbf{x}_{\text{scatter}}])$ and $\frac{\Delta T}{T}|_{\text{Doppler}} = \frac{2}{3}\hat{\mathbf{n}}' \cdot \nabla_{\mathbf{x}}\Phi[\mathbf{x}_{\text{scatter}}]/cH_0\sqrt{1+z}$, where $\mathbf{x}_{\text{scatter}} = D_A^{\text{co}}[z]\hat{\mathbf{n}}$, $\mathbf{x}_{\text{rec}} = \mathbf{x}_{\text{scatter}} + (D_A^{\text{co}}[z_{\text{rec}}] - D_A^{\text{co}}[z])\hat{\mathbf{n}}'$, $D_A^{\text{co}}[z] = 2\frac{c}{H_{e0}}\left(1 - \frac{1}{\sqrt{1+z}}\right)$. Here D_A^{co} is the comoving angular diameter distance, and the redshift of recombination, z_{rec} , will be approximated by ∞ for simplicity. The Hubble constant at the present time in the background cosmology, outside the void, is H_{e0} , whereas H_0 is the larger, present-day Hubble constant at the center

of the void.

We neglect the integrated Sachs-Wolfe (ISW) effect, meaning that a CMB photon does not contribute to the u -distortion simply because it passes across the void. This approximation is justified for a low-amplitude void in the EdS background where the ISW is a second-order effect. As Ω deviates from unity and/or the void amplitude becomes non-linear we expect a larger ISW contribution to the anisotropy and thus to the spectral distortion, but we do not expect that the ISW will ever be the dominant contributor to u for the small voids needed to mimic an accelerating universe.

The run of optical depth with redshift is taken from the unperturbed, background cosmology. We assume a rapid reionization at $z = z_{\text{rei}}$ such that $\frac{d\tau}{dz} = \tau'_{e0}\sqrt{1+z}\Theta[z_{\text{rei}}-z]$ $\tau'_{e0} = \frac{3H_{e0}\Omega_{b0}\sigma_{\text{T}}c}{8\pi Gm_{\text{H}}}\left(1 - \frac{1}{2}Y_{\text{He}}\right)$, where $\Theta[x]$ is the Lorentz-Heaviside step function, σ_{T} , m_{H} , Ω_{b0} , and Y_{He} are the Thomson cross-section, the hydrogen mass, the current baryonic mass density in units of the critical density, and the helium mass fraction, respectively. We use $\Omega_{b0}h^2 = 0.022$ ($h \equiv H_{e0}/100\text{km/s/Mpc}$), $Y_{\text{He}} = 0.24$. For H_0 we use the locally-measured expansion rate: 73 km/s/Mpc (*e.g.* Refs. [9, 10]). Where needed we use the WMAP3 [11] value, $\tau_{\text{obs}} = 0.9$, for the optical depth to the surface of last-scattering which in our model gives $z_{\text{rei}} = 11$. These numbers specify the cosmic evolution of the density of scatterers.

We assume spherical symmetry for the local void. Consequently, the gravitational potential is $\Phi[\mathbf{x}] = \Phi[R = |\mathbf{x}|]$, where R is the comoving radial distance from Earth. The temperature anisotropy $\Delta T/T$ depends on the directions $\hat{\mathbf{n}}$ and $\hat{\mathbf{n}}'$ only through the combination $\hat{\mathbf{n}} \cdot \hat{\mathbf{n}}'$, which leaves u $\hat{\mathbf{n}}$ -independent. Thus the final result is a single number, the u -distortion at Earth, which can be translated into a limit on any local spherical inhomogeneity.

Void Model: We cannot compute u for every possible void profile, so we focus our attention on a particularly simple, two parameter class of voids, sometimes known as a *Hubble bubble*: $\Phi[R] = \Phi_0\left(1 - \frac{R^2}{R_V^2}\right)\Theta[R_V - R]$. The parameters Φ_0 , R_V give the void amplitude and comoving radius. The reason it is called a Hubble bubble is that the Hubble parameter is uniform inside and outside the void, but the values differ. Nonlinear growth leads to the appearance of a shell of mass overdensity which compensates the underdensity in the void at the boundary of the outer and inner region. This compensating shell has a complicated density and velocity structure, which is safely ignored in linear theory. Away from the compensating shell this model resembles an open ($\Omega_0 < 1$) FRW cosmology embedded inside a flat EdS cosmology. Any smooth spherical void which is asymptotically EdS at large R and has finite density in the center can be thought of in this way; what differs is the radial profile of the transition between the two FRW spacetimes. The Hubble bubble is the limit of a sharp transition between

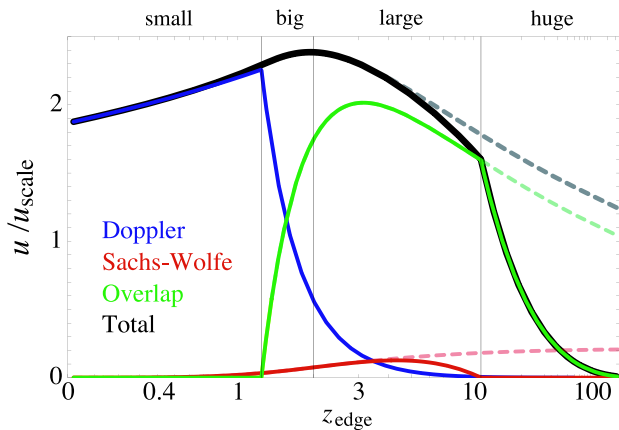


FIG. 2: The dependence of the spectral distortion, u , on the size of a Hubble bubble parameterized by z_{edge} , is shown in units of $u_{\text{scale}} \equiv \tau'_{e0} (\Phi_0/(3c^2))^2 (1+z_{\text{edge}})/(\sqrt{1+z_{\text{edge}}}-1)$. The thick curves show the various contributions to u . The dashed curves correspond to the case in which $z_{\text{rei}} \rightarrow \infty$. For small voids the Doppler contribution dominates, and the value of z_{rei} is unimportant.

the interior and exterior regions.

The Hubble bubble amplitude can be expressed in terms of the present-day density parameter, Ω_0 , inside the void as $\Phi_0 = \frac{3}{20} (H_{e0} R_V)^2 \left[\frac{(1-\Omega_0)^{3/2} H_0}{\Omega_0 H_{e0}} \right]^{2/3}$. Next, the void radius can be expressed as a function of the redshift at the edge of the void, z_{edge} . This relationship is complicated by finite peculiar velocities and non-linear clustering of the compensating shell, but to first order is simply $R_V = 2(c/H_0)(1 - 1/\sqrt{1+z_{\text{edge}}})$. Finally, the exterior Hubble parameter, H_{e0} , differs from the interior value, H_0 . At the same ‘‘time since bang’’ they are related as $\frac{H_0}{H_{e0}} = \frac{3}{2} \frac{\sqrt{1-\Omega_0} - \Omega_0 \sinh^{-1} \left[\sqrt{\frac{1-\Omega_0}{\Omega_0}} \right]}{(1-\Omega_0)^{3/2}}$. Note that a small jump in the Hubble parameter corresponds to a large jump in the density parameter (see fig. 3).

The gas at different redshift must satisfy several criteria in order to contribute to the u -distortion. A patch of gas at redshift z must be ionized, on our past light cone, and see an anisotropic ΔT from the void. We refer to the region $z > z_{\text{rei}}$ as the *neutral zone* because the gas is not ionized, producing no contribution to u . Even if the gas is ionized, if $z > z_{\text{max}} \equiv 3 + 4 z_{\text{edge}}$ then the gas is not in causal contact with the void so $\Delta T = 0$. We refer to the range $(2\sqrt{z_{\text{max}}+1}-1)/(\sqrt{z_{\text{max}}+1}-1)^2 \leq z \leq z_{\text{max}}$ as the *reflection zone*; the last scattering surface of gas in this range intersects the interior of the void so that, depending on the scattering angle, some CMB photons will reflect back towards us with anisotropy ΔT_{SW} . Gas which is on our past light cone and within the void will see $\Delta T_{\text{Doppler}}$, which we call the *Doppler zone*.

Five classes of void sizes are identified depending on how the different zones overlap (assuming $z_{\text{rei}} > 8$): *small* ($z_{\text{edge}} \leq \frac{5}{4}$) whereby the neutral zone, reflection zone, and Doppler zone are all disjoint; *big* ($\frac{5}{4} < z_{\text{edge}} \leq$

$\frac{1}{4}(z_{\text{rei}} - 3)$) whereby the Doppler zone and reflection zones overlap, but neither overlap the neutral zone; *large* ($\frac{1}{4}(z_{\text{rei}} - 3) < z_{\text{edge}} \leq z_{\text{rei}}$) in which the Doppler and reflection zones overlap, as do the reflection and neutral zones, but the neutral zone does not overlap the Doppler zone; *huge* ($z_{\text{edge}} > z_{\text{rei}}$) in which the neutral, reflection, and Doppler zones all overlap; and *super-horizon* ($R_V > 2c/H_0$) for which the void encompasses the entire observable universe. This classification is not restricted to the Hubble bubble void profile, but applies to any void profile with a sharp edge at $z = z_{\text{edge}}$. As we shall see it is only the small voids that can explain the current SNe data.

In the linear perturbation approximation for this void model the spectral distortion u is proportional to $(\frac{1}{3c^2} \Phi_0)^2 \tau_{e0}$ and may be decomposed as $u = \tau_{e0} (\frac{\Phi_0}{3c^2})^2 (U_D + U_S + U_{DS})$ where the three terms are, respectively, the contribution from gas where the temperature anisotropies are Doppler only (subscript D), Sachs-Wolfe only (subscript S), and a combination of the two (subscript DS). All of these can be expressed analytically. For small and big voids u does not depend on z_{rei} but only on the dimensionless size parameter $r \equiv \frac{1}{2} \frac{H_0}{c} R_V = 1 - \frac{1}{\sqrt{1+z_V}}$. The general expression for u is long and we do not give it here. For small voids, which are the most relevant, we find $U_D^{\text{small}} = \frac{28}{5} \frac{1}{r^3} \left(1 + \frac{1}{1-r} + \frac{2}{r} \ln[1-r] \right)$ and $U_S^{\text{small}} \ll U_D^{\text{small}}$ and $U_{DS}^{\text{small}} = 0$.

The angular-diameter distance D_A is a solution of the Dyer-Roeder [12] equation, $\frac{d}{dz} ((1+z)^2 H \frac{d}{dz} D_A) + \frac{3}{2} \Omega_H D_A = 0$. In the interior open and exterior flat cosmologies the respective solutions are $D_A[z < z_i] = \frac{2c}{H_0} (2 - \Omega_0(1-z) - (2 - \Omega_0)\sqrt{1+z\Omega_0})/(1+z)^2 \Omega_0^2$ and $D_A[z > z_e] = \frac{2c}{H_0} \left(\frac{C_1}{(1+z)} + \frac{C_2}{(1+z)^{3/2}} \right)$, where the coefficients C_1, C_2 are set by the continuity $D_A^{\text{int}}[z_i] = D_A^{\text{ext}}[z_e]$, and the jump in dD_A/dz as determined by integrating the Dyer-Roeder equation across the delta-function density spike at the void edge. The radial velocity drop, Δv , at the void edge means a double-valued $D_A[z]$ for $z \in [z_e, z_i]$ and $\frac{1+z_i}{1+z_e} = \sqrt{\frac{c+\Delta v}{c-\Delta v}}$. This drop also gives the Doppler anisotropy at the edge. To get z_i and z_e we use the approximations $\frac{\Delta v}{c} = \frac{\Delta T}{T}_{\text{Doppler}}[z_{\text{edge}}, \hat{\mathbf{n}}, \hat{\mathbf{n}}]$ and $z_{\text{edge}} = \frac{1}{2}(z_i + z_e)$. The luminosity distance versus redshift, a.k.a. the Hubble diagram, is $(1+z)^2 D_A[z]$.

Constraints: The u -distortion is evaluated according to the procedure described above. We are primarily interested in small and big voids which extend out to $z \sim 1$. Hence our constraints are independent of z_{rei} . The other cosmological parameters only enter into the overall normalization of u through τ'_{e0} . What remains are the void, size and amplitude: $(z_{\text{edge}}, \Omega_0)$.

The best current bound on u is due to FIRAS [13, 14, 15] which constrains $y < 15 \times 10^{-6}$ or $u < 3 \times 10^{-5}$ at 95% C.L.. The corresponding constraint on Hubble bubble parameters are shown in fig. 3. Also shown are

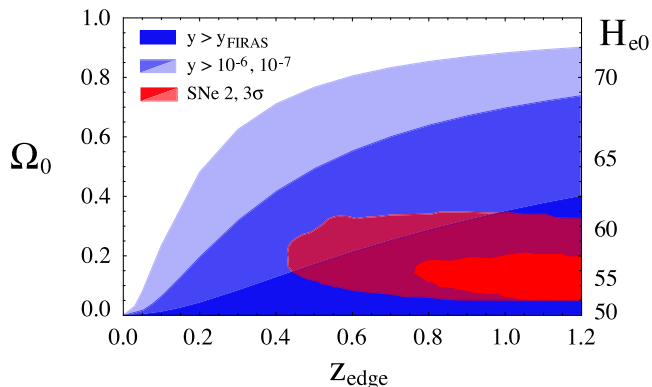


FIG. 3: The test of the Copernican Principle, in terms of constraints on the size and depth of a local, spherically-symmetric void, is shown. The blue shaded regions show the range of parameters excluded by the u -distortion test, whereas the red regions show the range of parameters compatible with the current SNe Hubble diagram data.

constraints for projected bounds $y < 10^{-6}, 10^{-7}$. The limits are expected to improve [16, 17], but a y -distortion from the IGM would likely mask the signal discussed here if $u \lesssim 10^{-6}$ [18].

The results rule out large voids with large density contrasts – the most egregious violations of the Copernican Principle. The larger the void, the smaller the density contrast must be in order to pass the test. Although not shown, the constraints become weaker for huge (nearly super-horizon sized) voids. Since observationally $\Omega_0 \lesssim 0.3$, only small bubbles with $z_{\text{edge}} < 0.9$ are allowed. Improving the constraint to $y < 10^{-6}$ would lower this bound to $z_{\text{edge}} \lesssim 0.3$ or a radius of 1 Gpc. These constraints are consistent with the very small Hubble bubble proposed in Ref. [19], with $H_0 - H_{e0} \sim 0.1H_0$ and $z_{\text{edge}} \gtrsim 0.025$.

The observed SNe data can be compared with our model Hubble diagram to further constrain void parameters. Using the SNe data [20, 21] compiled in Ref. [22], we computed the likelihood of Ω_0 and z_{edge} . The best-fit parameter combinations give $\chi^2 = 207$ for the 192 SNe magnitudes (within 3σ of the best-fit Λ CDM model based on a $\Delta\chi^2$ test, for a family of models with a sufficient number of parameters to encompass both Λ and the void). Voids which explain the observed Hubble diagram have low density and large size, $z_{\text{edge}} \sim 1$ (radii ~ 2.5 Gpc). However, as shown in fig. 3, combining the SNe data with current limits on u ($\chi^2 = 225, 250$ for 191 degrees of freedom), we find that nearly all such voids are ruled out. These specific constraints only apply to the Hubble bubble class of models, which also suffers from other flaws not mentioned here. This test will be applied to more general and more realistic void profiles.

An improvement in the bound on u by an order of magnitude may confirm or refute a wider variety of such voids as an explanation of the dark energy phenomena.

Yet, the u -distortion test presented here is more general than the question of dark energy. Future pursuit of this test will help improve our view of the universe on the largest scales.

We thank the Galileo Galilei Institute for Theoretical Physics for the hospitality and the INFN for partial support during the completion of this work. R.C. was supported in part by NSF AST-0349213 at Dartmouth and A.S. by the DoE at Fermilab.

-
- [1] S. Perlmutter *et al.* [Supernova Cosmology Project Collaboration], *Astrophys. J.* **517**, 565 (1999).
 - [2] A. Riess *et al.* [Supernova Search Team Collaboration], *Astron. J.* **116**, 1009 (1998).
 - [3] A. Hajian and T. Souradeep, *Phys. Rev. D* **74**, 123521 (2006); T. R. Jaffe, *et al.*, *Astrophys. J.* **629**, L1 (2005).
 - [4] D. W. Hogg, *et al.*, *Astrophys. J.* **624**, 54 (2005).
 - [5] M. N. Celerier, *Astron. Astrophys.* **353**, 63 (2000); R. K. Barrett and C. A. Clarkson, *Class. Quant. Grav.* **17**, 5047 (2000); K. Tomita, *Mon. Not. R.A.S.* **326**, 287 (2001); K. Tomita, *Prog. Theor. Phys.* **106**, 929 (2001); H. Iguchi, T. Nakamura and K. I. Nakao, *Prog. Theor. Phys.* **108**, 809 (2002); J. W. Moffat, *JCAP* **0605**, 001 (2006); H. Alnes, M. Amarzguioui and O. Gron, *Phys. Rev. D* **73**, 083519 (2006); R. Mansouri, arXiv:astro-ph/0512605; C. H. Chuang, J. A. Gu and W. Y. Hwang, arXiv:astro-ph/0512651; R. A. Vanderveld, E. E. Flanagan and I. Wasserman, *Phys. Rev. D* **74**, 023506 (2006); D. Garfinkle, *Class. Quant. Grav.* **23**, 4811 (2006); R. Mansouri, arXiv:astro-ph/0606703; D. J. H. Chung and A. E. Romano, *Phys. Rev. D* **74**, 103507 (2006); K. Enqvist and T. Mattsson, *JCAP* **0702**, 019 (2007); H. Alnes and M. Amarzguioui, *Phys. Rev. D* **75**, 023506 (2007); M. N. Celerier, [arXiv:astro-ph/0702416].
 - [6] H. Bondi, *Mon. Not. Roy. Astron. Soc.* **107**, 410 (1947).
 - [7] A. Stebbins, arXiv:astro-ph/0703541.
 - [8] J. Chluba and R. A. Sunyaev, *Astron. Astrophys.* **424**, 389 (2003).
 - [9] W. L. Freedman *et al.*, *Astrophys. J.* **553**, 47 (2001).
 - [10] A. G. Riess *et al.*, *Astrophys. J.* **627**, 579 (2005).
 - [11] D.N. Spergel, R. Bean, *et al.*, *Astrophys. J. Suppl.* **170**, 377 (2007).
 - [12] C. Dyer and R. Roeder, *Astrophys. J.* **180** 31 (1973).
 - [13] J. C. Mather, *et al.*, *Astrophys. J.* **420**, 439 (1994).
 - [14] N.W. Boggess, J.C. Mather, R. Weiss *et al.*, *Astrophys. J.* **397**, 420 (1992).
 - [15] D. Fixsen, E. Cheng, *et al.*, *Astrophys. J.* **473**, 576 (1996).
 - [16] D. J. Fixsen and J. C. Mather, *Astrophys. J.* **581**, 817 (2002).
 - [17] A. Kogut *et al.*, *New Astron. Rev.* **50**, 925 (2006).
 - [18] J. Zhang, U. Pen and H. Trac, *Mon. Not. Roy. Astron. Soc.* **355** 451 (2004).
 - [19] S. Jha, A. G. Riess and R. P. Kirshner, *Astrophys. J.* **659**, 122 (2007).
 - [20] A. G. Riess *et al.*, *Astrophys. J.* **659** 98 (2007).
 - [21] W. M. Wood-Vasey *et al.*, *Astrophys. J.* **666** 694 (2007).
 - [22] T. M. Davis *et al.*, *Astrophys. J.* **666** 716 (2007).